

Strain-induced insulator state in $\text{La}_{0.7}\text{Sr}_{0.3}\text{CoO}_3$

A. D. Rata¹, A. Herklotz¹, K. Nenkov^{1,2}, L. Schultz¹, and K. Dörr¹

¹*IFW Dresden, Institute for Metallic Materials, Helmholtzstraße 20, 01069 Dresden, Germany*

²*International Laboratory of High Magnetic Fields and Low Temperatures, PL-53421 Wrocław, Poland*

(Dated: February 5, 2008)

We report on the observation of a strain-induced insulator state in ferromagnetic $\text{La}_{0.7}\text{Sr}_{0.3}\text{CoO}_3$ films. Tensile strain above 1% is found to enhance the resistivity by several orders of magnitude. Reversible strain of 0.15% applied using a piezoelectric substrate triggers huge resistance modulations, including a change by a factor of 10 in the paramagnetic regime at 300 K. However, below the ferromagnetic ordering temperature, the magnetization data indicate weak dependence on strain for the spin state of the Co ions. We interpret the changes observed in the transport properties in terms of a strain-induced splitting of the Co e_g levels and reduced double exchange, combined with a percolation-type conduction in an electronic cluster state.

The electronic properties of some transition metal (TM) oxide compounds are highly sensitive to external parameters such as magnetic and electric fields, pressure, and chemical doping. One prominent example are the manganese perovskites $\text{R}_{1-x}\text{A}_x\text{MnO}_3$ showing the colossal magnetoresistance (CMR) phenomenon, where $\text{R} = \text{La}$ or a rare earth metal and $\text{A} = \text{non-trivalent metal}$ ^{1,2,3}. The width (W) of the TM $3d$ bands is typically low in these materials and, thus, electronic transport is susceptible to localization effects. W can be modified by changing the TM-oxygen bond lengths and/or the TM-O-TM bond angles. Hence, hydrostatic pressure as well as epitaxial strain in thin films may affect strongly the electronic structure and transport properties. Beside the necessity to clarify the influence of strain for applications of TM oxides in microelectronics, controlled strain may provide an efficient tool to tune their electronic properties.

Recently, a strong sensitivity to pressure has been revealed for cobaltites, e.g., in $\text{La}_x\text{Sr}_{1-x}\text{CoO}_3$ ^{4,5,6}. The conductivity of $\text{La}_{0.82}\text{Sr}_{0.18}\text{CoO}_3$ single crystals was found to decrease under pressure, although intuitively the width of the conduction bands is expected to increase with pressure. A pressure-induced insulator state has been observed and attributed to a pressure-induced transition to a low-spin state for the Co^{3+} ions^{4,5}. Perovskite-type cobaltites possess thus an additional degree of freedom: the $\text{Co}^{3+} d^6$ and $\text{Co}^{4+} d^5$ ions may display various spin states. This is due to a delicate balance between the crystal-field splitting Δ_{CF} and the intraatomic Hund exchange J_{H} ⁷. Since Δ_{CF} is very sensitive to the variation of the Co-O bond length^{8,9}, structural changes may be used to modify the ratio between Δ_{CF} and J_{H} .

The ground state of the parent compound LaCoO_3 is nonmagnetic with a low-spin (LS, $S = 0$) configuration, which can be thermally excited either to an intermediate-spin (IS, $S = 1$) or a high-spin (HS, $S = 2$) state above $T \sim 100 \text{ K}$ ^{7,9}. By doping with Sr^{2+} , the material turns into a ferromagnetic cluster-glass for $x > 0.18$, following a spin-glass-like region between $x = 0$ and $x = 0.18$ ^{10,11}. In the simplest picture, doping is associated with the creation of Co^{4+} ions and the double exchange (DE) between Co^{4+} and the adjacent IS Co^{3+} induces ferromag-

netic couplings^{11,12}. The electrical conductivity increases with x and for $x \geq 0.20$ the system is metallic^{10,11,13,14}.

Here, we investigate the influence of epitaxial strain on the electronic transport and magnetization of $\text{La}_{0.7}\text{Sr}_{0.3}\text{CoO}_3$ films epitaxially grown on various substrates. The strain drastically modifies the conductivity of our films, by several orders of magnitude. An insulator-type behavior is observed in films grown under tensile strain, whereas compressed films show bulk-like, metallic properties. Nevertheless, the magnetiza-

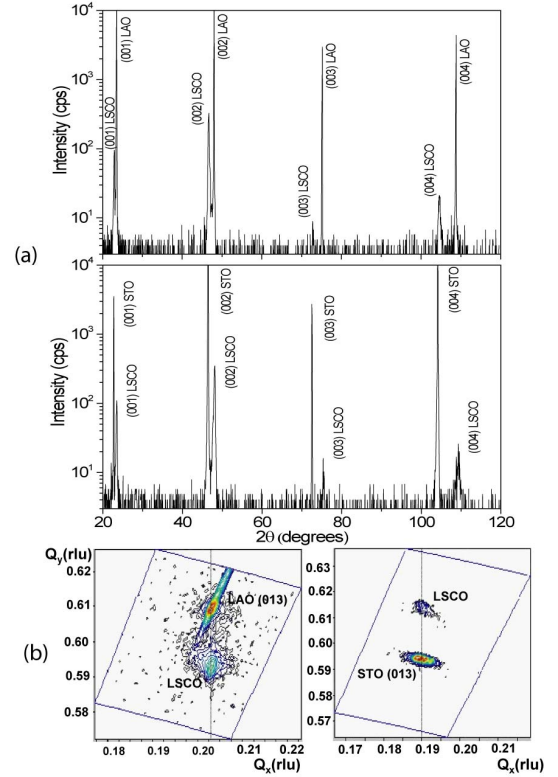


FIG. 1: 1a) $\Theta - 2\Theta$ X-ray diffractograms of 60 nm thick LSCO films, grown on LAO (top) and STO (bottom) substrates. 1b) XRD reciprocal space map around the (013) reflection for LSCO films on LAO (left) and STO (right).

TABLE I: In-plane a and out-of-plane c lattice parameters of the LSCO films, their tetragonal distortion t defined as $2(a - c)/(a + c)$, and the Curie temperature T_C . The lattice parameter (a_{sub}) of each substrate is also given.

LSCO films (60 nm)	a_{sub} (Å)	c (Å)	a (Å)	t	T_C (K)
LSCO/LAO	3.78	3.87	3.78	-2.3%	194
LSCO/STO	3.905	3.78	3.90	+3.1%	195
LSCO/PMN-PT	4.02	3.79	3.86	+1.8%	200

tion data reveal a much weaker response to the strain, with rather small changes of the ordered magnetic moments and ordering temperature T_C . The dependence on strain of the resistance and magnetization of the $\text{La}_{0.7}\text{Sr}_{0.3}\text{CoO}_3$ films was also measured by dynamic strain experiments, using a pseudocubic piezoelectric substrate. Once again, an extreme effect of strain on the transport is found, while only minor changes of the magnetization were observed. We discuss the experimental results in terms of a strain-induced splitting of the Co e_g levels and reduced DE, combined with a percolation-type conduction in an electronic cluster state.

$\text{La}_{0.7}\text{Sr}_{0.3}\text{CoO}_3$ (LSCO) films were grown on single-crystalline substrates of $\text{SrTiO}_3(001)$ (STO), $\text{LaAlO}_3(001)$ (LAO), and $\text{Pb}(\text{Mg}_{1/3}\text{Nb}_{2/3})_{0.72}\text{Ti}_{0.28}\text{O}_3(001)$ (PMN-PT) by pulse laser deposition (KrF 248 nm) from a stoichiometric target. The deposition temperature and the oxygen background pressure were 650°C and 3.5×10^{-1} mbar, respectively. After deposition, the films were cooled down in oxygen atmosphere of 600 mbar. The deposition rate was calibrated by measuring the film thickness by X-ray reflectivity. X-ray diffraction (XRD) measurements for structural characterization were carried out in a Philips XPert MRD diffractometer using Cu $K\alpha$ radiation. The surface microstructure of the films was probed by Atomic Force Microscopy (AFM). The magnetization M was measured in a SQUID magnetometer in both field-cooled (FC) and zero-field cooled (ZFC) modes. Electrical transport measurements using a standard four-point technique were performed either with a Quantum Design PPMS system or a split-coil magnet. In recent work^{15,16} we have proposed the reversible control of the biaxial in-plane strain in films grown epitaxially on piezoelectric PMN-PT(001). The substrate strain is controlled by applying an electrical voltage between the conducting film and a bottom electrode on the opposite face of the substrate (see inset in Fig. 4a). The employed PMN-PT has a rhombohedral lattice structure similar to that of LAO, apart from the larger lattice parameter of 4.02 Å. If the LSCO films had too high resistance for the proper function as an electrode, Pt electrodes were deposited on top, which allows a two-point measurement of the LSCO resistance.

First, structural results for LSCO films grown epitax-

ially in three distinct strain states, induced by varying the substrate lattice parameter, will be discussed. In Fig. 1a we show the wide angle $\Theta - 2\Theta$ diffractograms of 60 nm thick films grown on LAO (top) and STO (bottom) substrates. The films display clear (001) reflections of the pseudocubic perovskite structure, which are substantially shifted by the induced strain. The LSCO film grown on LAO (STO) is under in-plane compressive (tensile) strain. No impurity phase or deviating orientations were detected. In Fig. 1b we compare the XRD reciprocal space maps around the non-specular (013) reflection of LSCO films grown on LAO and STO substrates. The intensity scale in the figure is logarithmic. The horizontal and vertical axes are Q-vectors parallel (Q_x) and perpendicular (Q_y) to the surface plane, respectively. In each case, the XRD peaks of the LSCO film and the substrate, either LAO or STO, are observed at the same Q_x values, proving that the growth is coherent. The derived pseudocubic in-plane lattice parameters of the films are 3.78 Å and 3.90 Å for the LAO and STO substrates, respectively, whereas the value for bulk LSCO is 3.82 Å¹³. In Table 1, the in-plane (a) and out-of-plane (c) lattice parameters of three different films and their tetragonal distortion estimated as $t = 2(a - c)/(a + c)$ are listed. The third film, i.e., LSCO/PMN-PT, is epitaxially oriented but not coherently grown. This film is used to study the response to the reversible strain applied by the piezoelectric substrate. The tetragonal distortion of the three films spans a wide range, from -2.3% (LAO) to 1.8% (PMN-PT) and 3.1% (STO).

A drastic effect of the epitaxial strain is observed in the electrical transport of the LSCO films. In Fig. 2, we present the temperature dependence of the resistivity (ρ) of LSCO films in different strain states. Clearly, the LSCO/PMN-PT film with medium tensile strain displays an insulating-type behaviour. Further, the LSCO/STO film had a Giga-ohm resistance even at 300 K. In contrast, the LSCO/LAO film displays metallic conductivity at all temperatures, which is similar to the bulk behaviour^{11,14,17,18}. At 5 K, for example, the resistivity is $\rho \simeq 1.2 \times 10^{-4} \Omega \text{ cm}$. We argue that this strikingly large conductivity variation among the different films is essentially caused by the varied strain state. The possibility of having non-connected films or microcracks as origin of the insulating behaviour can clearly be ruled out from the AFM images, which show fairly smooth films with a roughness (rms) of about 1 nm. Further, any kind of extended defects capable to interrupt the current path would lead to strain relaxation, which is absent for the film on STO.

Unlike the striking differences observed in the electrical transport, the impact of biaxial strain on the magnetic ordering is astonishingly moderate. The temperature-dependent magnetization of the LSCO/LAO and LSCO/STO films is plotted in Fig. 3. The data were recorded during warming in a magnetic field of 100 mT applied along the [100] in-plane direction for both FC and ZFC runs. Interestingly, the magnetic ordering sets

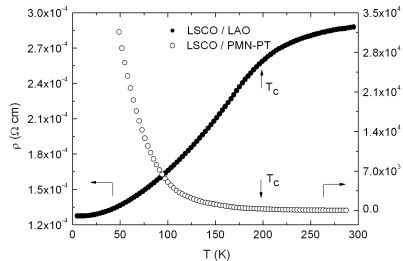


FIG. 2: Temperature dependence of the resistivity of LSCO / LAO (left scale) and LSCO / PMN-PT (right scale) 60 nm thick films.

in at about 210 K, irrespective of the strain state. The ferromagnetic Curie temperature (T_C) estimated by extrapolating M^2 for $T < T_C$ to $M = 0$ is given in Table 1. The T_C values are somewhat lower as compared to the single-crystal bulk value, i.e., 225 K^{14,17}, but are in agreement with those reported by Fuchs *et al.* for low-strain films¹⁹. The lower T_C of our films can be then associated with finite size, thickness effect²⁰. A pronounced branching between the ZFC and FC curves is observed (Fig. 3), indicating a lack of long-range ferromagnetic order and the presence of magnetic clusters in a cluster-glass state^{10,11}. Although there is no significant difference in the FC curves of the two films, a higher ZFC magnetization is observed for the LSCO/LAO film. This points to stronger inter-cluster ferromagnetic interactions in this film. In the framework of the DE ferromagnetism, this observation is in line with the metallic character of the LSCO/LAO film.

We recorded the magnetization of a 30 nm thick LSCO/PMN-PT film as a function of a gradually increasing in-plane piezo-compression which relaxes the as-grown tensile strain. A continuous increase of M is observed near T_C , as shown in the inset of Fig. 4b. Therefore, the increase of M results from the reduced tetragonal distortion of the unit cell. Interestingly, this is analogue to the strain effect on M in $\text{La}_{0.7}\text{Sr}_{0.3}\text{MnO}_3$ ¹⁵, where the ferromagnetism originates from the DE mechanism. In Fig. 4b we show the temperature dependence of the relative change of M obtained by applying an electric field of 14 kV/cm to the substrate. This electric field produces an in-plane compression of 0.15% at 300 K and a slightly weaker one at lower temperatures. As for the manganites¹⁵, the strain response peaks near T_C and vanishes for $T \ll T_C$.

Transport data measured as function of the reversibly applied piezoelectric substrate strain give direct evidence for the extreme sensitivity to strain of the LSCO films. In Fig. 4a we plot the resistance R vs. the electric field applied to the substrate, recorded at room temperature in a slow run, taking one hour. It is highly hysteretic and reveals a reversible R modulation by a factor of 10. In order to exclude charging effects the R vs strain measure-

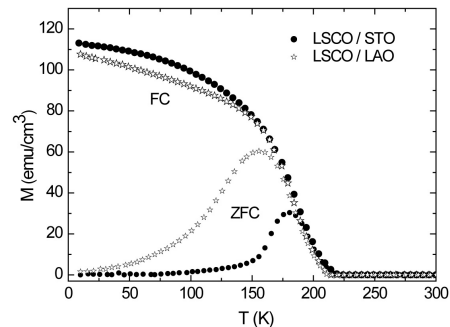


FIG. 3: Magnetization of LSCO films as a function of temperature measured both in FC and ZFC mode, with a field of 100 mT along the [100] pseudocubic substrate direction.

ments were performed at various speeds. Similar data recorded near T_C show a modulation of R by a factor of $\simeq 3$. Apart from the much larger magnitude of the effect, the decrease of R upon release of tensile strain (i.e., reduced tetragonality of the unit cell) agrees again with the observations for $\text{La}_{0.7}\text{Sr}_{0.3}\text{MnO}_3$ films¹⁶. Further, it is important to note that the strain effect we observe at 300 K appears far above T_C , in the paramagnetic range.

Tensile strain is known to induce an insulator state in thin films of ferromagnetic metallic manganites^{3,21,22}. For $\text{La}_{0.7}\text{Sr}_{0.3}\text{CoO}_3$, the mechanisms already invoked for manganites seem to play an important role, too, and will be discussed in the next paragraph. First, the implications of a possible spin-state transition for the Co ions is considered. The observed pressure-induced insulating state in $\text{La}_{0.82}\text{Sr}_{0.18}\text{CoO}_3$ is related to an enhancement of the crystal-field splitting, driving Co^{3+} ions into the LS state and depleting the e_g conduction-band^{4,5}. This mechanism is unlikely to be the origin of the insulator state induced by tensile strain in our films. The enlarged in-plane lattice parameter in our LSCO/STO films is expected to reduce the splitting of the Co t_{2g} and e_g levels. Additionally, the tetragonal distortion would split the e_g and t_{2g} levels and result in a further reduction of the t_{2g} - e_g energy separation. Tensile strain can thus induce a larger number of excited Co ions in the film, in contrast to hydrostatic pressure. Still, for the doping level, $x = 0.3$, and range of temperatures, $T < T_C$, we investigated, the spin state of the Co ions seems to be rather insensitive to strain. This is supported by the observed weak dependences of M , see Fig. 3, and of the saturated magnetization on strain. Further, M increases when reducing the tensile strain, see Fig. 4b, contrary to the expectation for a strain-induced IS or HS Co spin state.

Phase separation into hole-rich metallic ferromagnetic clusters and insulating, magnetically less-ordered regions is widely accepted for $\text{La}_{1-x}\text{Sr}_x\text{CoO}_3$ with $x < 0.5$ ^{12,13,18,23,24}. Magnetic field or pressure induced cluster percolation may trigger extreme changes of the electrical conductivity, as seen in colossal magnetoresistive manganites^{1,2}. A percolation scenario could also under-

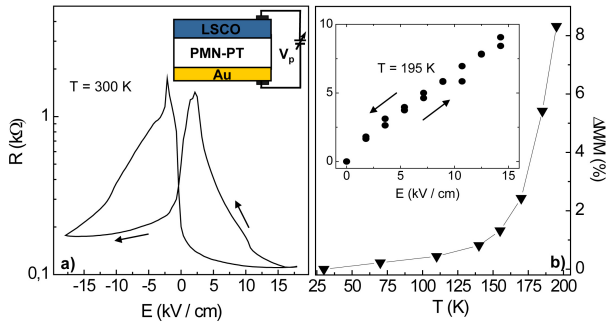


FIG. 4: (a) Resistance vs the electric field applied to the substrate for a 60 nm LSCO/PMN-PT(001) film ($E/[001]$). Inset shows the schematic device structure. (b) Maximum change of M calculated as $[M(E) - M(0)]/M(0)$ at various temperatures for $E = 14$ kV/cm and a 30 nm thick film. Inset shows the change of M (in percent) with electric field, recorded at 195 K.

lie the huge difference in conductivity for our differently strained films as well as the extremely large direct strain effect (Fig. 4a). The observation of the latter at 300 K goes beyond the characteristics of the CMR manganites because it occurs in the paramagnetic state, indicating the existence of an electronic cluster state at $T \gg T_C$. The magnetization data (Fig. 3) resemble the characteristics of a cluster state as typically observed in the bulk. Furthermore, we found a strong increase of the coercive field for the LSCO/STO (879 mT at 10 K) as compared to LSCO/LAO (440 mT at 10 K). This points to weaker inter-cluster coupling in the LSCO/STO film, which is in line with the insulating state. A phase separation scenario could also explain the strikingly weak change of T_C with strain. It seems that T_C is mainly determined by the intra-cluster ordering. At this point it is worth noting the rather weak dependence of T_C with doping, i.e., $220 \text{ K} < T_C < 270 \text{ K}$, in bulk $\text{La}_{1-x}\text{Sr}_x\text{CoO}_3$ with x varying between 0.2 and 0.9^{11,25}, which may as well be related to a magnetic phase separation.

At the microscopic level, the strain effect in ferromagnetic manganites has been essentially attributed to changes in the ferromagnetic DE and the Jahn-Teller splitting of the e_g levels^{1,2,3}. In nearly cubic compounds, the strain-induced tetragonal distortion of the unit cell produces (i) a suppression of the DE mechanism and (ii) static Jahn-Teller type distortions favoring the occupation of the in-plane $e_g d_{x^2-y^2}$ orbitals^{21,22,26}. Both effects lead to electron localization. A similar interplay

between the DE and strain-induced Jahn-Teller/orbital ordering may be active in cobaltites and could be responsible for the observed strain-induced insulator state in $\text{La}_{0.7}\text{Sr}_{0.3}\text{CoO}_3$. This idea is supported by the fact that the same dependences were found with strain for both magnetization and resistance in the direct-strain experiments on $\text{La}_{0.7}\text{Sr}_{0.3}\text{MnO}_3$ and $\text{La}_{0.7}\text{Sr}_{0.3}\text{CoO}_3$: reduced tetragonality leads to larger magnetization and lowers the resistivity. On the other hand, the electronic structure and, thus, transport properties in cobaltites may be even more sensitive to structural changes as compared to the manganites. Reliable *ab initio* calculations are strongly desirable to clarify these issues. Additionally, cobaltites may offer access to strain-induced control of electronic properties in the paramagnetic range at temperatures above 300 K.

Finally, it is ruled out that compositional differences among the films cause the different conductivity. Tensile strain could result in oxygen deficiency and/or Sr enrichment. In bulk, oxygen vacancies up to 5% lead to an increase of R by less than a factor of 5²⁷. Higher Sr doping would drive the films metallic according to the bulk phase diagram. Considering also the huge direct resistive strain effect, we argue that composition is unlikely to be responsible for the observed variation of the conductivity.

To summarize, the effects of both static and dynamic biaxial strain on electrical transport and magnetization of $\text{La}_{0.7}\text{Sr}_{0.3}\text{CoO}_3$ films have been investigated. Depending on the strain state, we observed extreme changes in the conductivity. In particular, tensile strain above 1% is found to induce a transition to an insulator state. Reversible strain of 0.15% triggered huge resistance modulations, including a change by a factor of 10 in the paramagnetic regime at 300 K. Whereas epitaxial strain may generally be applied to control the spin state in cobaltite films due to their small crystal field splitting, the weak dependence of the magnetization on strain indicates only a minor modification of the spin state in $\text{La}_{0.7}\text{Sr}_{0.3}\text{CoO}_3$ below T_C . We interpret the changes observed in the transport properties in terms of a strain-induced splitting of the Co e_g levels and reduced double exchange, combined with a percolation-type conduction in an electronic cluster state.

We would like to thank D. Khomskii, M. Richter, L. Hozoi, V. Kataev, K. H. Müller, H. Tjeng and L. Eng for fruitful discussions and C. Richter for the help with electrical measurements. This work was supported by Deutsche Forschungsgemeinschaft, FOR 520.

¹ Y. Tokura, Rep. Prog. Phys. **69** 797851 (2006).

² E. Dagotto, T. Hotta, and A. Moreo, Phys. Rep. **344**, 1 (2001).

³ K. Dörr, J. Phys. D **39**, R125-R150 (2006).

⁴ R. Lengsdorf, M. Ait-Tahar, S. S. Saxena, M. Ellerby, D. I. Khomskii, H. Micklitz, T. Lorenz, and M. M. Abd-

Elmeguid, Phys. Rev. B **69**, 140403 (2004).

⁵ R. Lengsdorf, J. -P. Rueff, G. Vank, T. Lorenz, L. H. Tjeng, and M. M. Abd-Elmeguid, Phys. Rev. B **75**, 180401 (2007).

⁶ I. Fita, R. Szymczak, R. Puzniak, I. O. Troyanchuk, J. Fink-Finowicki, Ya. M. Mukovskii, V. N. Varyukhin, and H. Szymczak, Phys. Rev. B **71**, 214404 (2005).

- ⁷ P. M. Raccah and J. B. Goodenough, *Phys. Rev.* **155**, 932 (1967).
- ⁸ D. M. Sherman, in *Advances in Physical Geochemistry*, edited by S. K. Saxena (Springer-Verlag, Berlin, 1988).
- ⁹ M. A. Korotin, S. Yu. Ezhov, I. V. Solovyev, V. I. Anisimov, D. I. Khomskii, and G. A. Sawatzky, *Phys. Rev. B* **54**, 5309 (1996).
- ¹⁰ Masayuki Itoh, Ikuomi Natori, Satoshi Kubota and Kiyochiro Motoya, *J. Phys. Soc. Jpn.* **4**, 1486 (1994).
- ¹¹ M. A. Senaris-Rodriguez and J. B. Goodenough, *J. Solid State Chem.* **118**, 323 (1995).
- ¹² D. Louca, and J. L. Sarrao, *Phys. Rev. Lett.* **91**, 155501 (2003).
- ¹³ R. Caciuffo, D. Rinaldi, G. Barucca, J. Mira, J. Rivas, M. A. Se  naris-Rodr  guez, P. G. Radaelli, D. Fiorani, and J. B. Goodenough, *Phys. Rev. B* **59**, 1068 (1999).
- ¹⁴ M. Kriener, C. Zobel, A. Reichl, J. Baier, M. Cwik, K. Berggold, H. Kierspel, O. Zabara, A. Freimuth, and T. Lorenz, *Phys. Rev. B* **69**, 094417 (2004).
- ¹⁵ C. Thiele, K. D  rr, O. Bilani, J. R  del, and L. Schultz, *Phys. Rev. B* **75**, 054408 (2007).
- ¹⁶ R. B. Gangineni, L. Schultz, C. Thiele, I. M  nch, and K. D  rr, *Appl. Phys. Lett.* (in press).
- ¹⁷ H. M. Aarbhog, J. Wu, L. Wang, H. Zheng, J. F. Mitchell, and C. Leighton, *Phys. Rev. B* **74**, 134408 (2006).
- ¹⁸ M. J. R. Hoch, P. L. Kuhns, W. G. Moulton, A. P. Reyes, M. A. Torija, J. F. Mitchell, and C. Leighton, *Phys. Rev. B* **75**, 104421 (2007).
- ¹⁹ D. Fuchs, O. Mor  n, P. Adelman, and R. Schneider, *Physica B* **349**, 337 (2004).
- ²⁰ D. Fuchs, T. Schwarz, O. Mor  n, P. Schweiss, and R. Schneider, *Phys. Rev. B* **71**, 092406 (2005).
- ²¹ Yafeng Lu, J. Klein, F. Herbstritt, J. B. Philipp, A. Marx, and R. Gross, *Phys. Rev. B* **73**, 184406 (2006).
- ²² M. Ziese, H. C. Semmelhack, and K. H. Han, *Phys. Rev. B* **68**, 134444 (2003).
- ²³ J. Wu, J. W. Lynn, C. J. Glinka, J. Burley, H. Zheng, J. F. Mitchell, and C. Leighton, *Phys. Rev. Lett.* **94**, 037201 (2005).
- ²⁴ D. Phelan, D. Louca, S. Rosenkranz, S. -H. Lee, Y. Qiu, P. J. Chupas, R. Osborn, H. Zheng, J. F. Mitchell, J. R. D. Copley, J. L. Sarrao, and Y. Moritomo, *Phys. Rev. Lett.* **96**, 027201 (2006).
- ²⁵ J. E. Sunstrom IV, K. V. Ramanujachary, M. Greenblatt, and M. Croft, *J. Solid State Chem.*, **139**, 388 (1998).
- ²⁶ Z. Fang, I. V. Solovyev, and K. Terakura, *Phys. Rev. Lett.* **84**, 3169 (2000).
- ²⁷ Hai-Wen Hsu, Yen-Hwei Chang, and Guo-Ju Chen, *Jpn. J. Appl. Phys.* **39**, 61 (2000).